CONFERENCE PRE-PRINT

DEVELOPMENT AND EXPERIMENTAL PROGRESS OF KTX REVERSED FIELD PINCH

Ge Zhuang[1], Wenzhe Mao[1*], Tao Lan[1*], Jinlin Xie[1], Hong Li[1], Ahdi Liu[1], Zhengwei Wu[1], Caoxiang Zhu[1], Chu Zhou[1], Zixi Liu[1], Hai Wang[1], Zian Wei[1], Xiaohui Wen[1], Haiyang Zhou[1], Yolbarsop Adil[1], Jie Wu[1], Yinan Zhou[1], Yiming Zu[1], Shoubiao Zhang[2], Yingqiao Wang[3], Haifeng Liu[4], Chijin Xiao[1,5], Weixing Ding[1,6] and Wandong Liu[1]

[1] School of Nuclear Science and Technology, University of Science and Technology of China, Hefei 230026, China
[2] Institute of Plasma Physics, Chinese Academy of Sciences, Hefei 230031, China
[3] Southwestern Institute of Physics, P.O. Box 432, Chengdu 610041, China
[4] School of Physical Science and Technology, Southwest Jiaotong University, Chengdu 610031, China
[5] Plasma Physics Laboratory, University of Saskatchewan, Saskatoon, Saskatchewan, SK 7N 5E2, Canada
[6] University of California Los Angeles, Department of Physics, Los Angeles, California 90095, USA

Email: maozhe@ustc.edu.cn, lantao@ustc.edu.cn

Abstract

Keda Torus eXperiment (KTX), a Reversed Field Pinch (RFP) device, has undergone upgrades to advance fusion research. The operational enhancements include an upgraded Ohmic field which has enabled high-current discharges over 500 kA and the development of a boundary magnetic field feedback control system to extend discharge durations and improve confinement towards a Quasi-Single Helicity (QSH) state in the future. Additionally, a Compact Toroidal Injection (CTI) system has been successfully tested, achieving CT plasma injection at speeds up to 300 km/s to enhance core fueling and plasma density control. New diagnostic systems, such as a terahertz polarimetric interferometer, and a double-foil soft X-ray diagnostic system, have been applied to do equilibrium reconstruction and study plasma instabilities. Furthermore, numerical simulations have provided theoretical support by exploring the maintenance mechanisms of the QSH state. These studies have highlighted the role of helicity in magnetic topology, the importance of drift flows in plasma self-organization, and the distinct non-axisymmetric field distribution of the QSH state. These comprehensive upgrades and studies on KTX lay a solid foundation for future magnetic confinement fusion experiments in RFP configuration.

1. INTRODUCTION

KTX Reversed Field Pinch (RFP) device [1] has undergone several key upgrades in recent years to enhance its operational capabilities and provide new experimental and theoretical support for in-depth research on RFP physics. Through these modifications, KTX aims to achieve discharge operations under higher confinement regimes and conduct three-dimensional physics research.

In terms of power for magnetic field coils, firstly, the Ohmic field power energy has been upgraded, and higher toroidal plasma current discharges have been achieved, with the maximum plasma current over 500 kA. Secondly, the development of a boundary magnetic field feedback control system [2] has improved plasma confinement performance, and extended discharge durations, aiming for QSH state regulation. This system monitors changes in magnetic fields and plasma using sensors including eddy current probes [3], and in combination with error field feedback coils at the vertical gaps and saddle coils with independent power supplies [4], can enhance plasma stability and confinement.

In terms of assisted control systems, an electron cyclotron wave (ECW) is applied for pre-ionization at the present stage, and it is expected to exploring non-inductive current driven scheme for magnetic fluctuation suppression. Two bias electrodes are employed for boundary electric field control [5], which can further adjust edge current density profile and plasma flow for optimizing confinement performance. KTX has also conducted research on the Compact Toroidal Injection (CTI) system [6], successfully achieving CT plasma injection with maximum speed approaching 300km/s, which can enhance fueling capacity and improve plasma density control. This system can effectively penetrate the magnetic field and diffuse into the plasma core. In experiments, other effects caused by this system were also discovered, such as the excitation of Alfven waves and the injection of helicity. This provides new technical support for future magnetic confinement fusion experiments.

Based on the upgraded ohmic field power supply, the duration of high loop voltage was extended, and we achieved a maximum discharge current of 500 kA in ultra-low q configurations. Using the active feedback control power supply, we can generate a vertical magnetic field component, achieving discharges lasting several times the shell time in tokamak mode. By adjusting the inductance of toroidal coils, we realized RFP discharges in the aided reversal mode. The flexible operational scenarios provide the necessary conditions for conducting common physics research on KTX in different magnetic configurations.

Regarding diagnostic capabilities, KTX has developed a series of advanced diagnostic systems aimed at studies of anomalous transport behavior and quasi-single helicity (QSH) states in the reverse field pinch plasma. Key diagnostic achievements include: a fast-scanning electromagnetic probe system for high-time resolution measurement of electromagnetic fluctuations at the plasma edge, a terahertz solid-state source polarimetric interferometer system for high-precision density measurement and magnetic field fluctuation analysis [7], revealing electron density and internal magnetic field dynamics of the plasma, and a double-foil soft X-ray diagnostic system for precise imaging of the plasma's helical structure. These diagnostic methods would provide crucial experimental data for understanding the physical behavior of reverse field pinch plasmas.

In terms of physical research, numerical simulations have explored the characteristics and maintenance mechanisms of the QSH state in the RFP device from three aspects [8]. The study indicates that the helicity's impact on the magnetic topology is a key factor, and the formation of the QSH state helps to improve energy confinement. Simulations of electrostatic drift reveal the important role of drift flows in maintaining the QSH state, enhancing the plasma's self-organization ability [9]. Moreover, three-dimensional equilibrium reconstruction analysis has revealed the non-axisymmetric magnetic field distribution in the QSH state and its distinct characteristics compared to the multi-helicity (MH) state [10]. Those results are expected to provide important theoretical support for understanding and optimizing the three-dimensional state in RFP devices.

As an alternative magnetic confinement fusion reactor concept, the Reversed-Field Pinch (RFP) has unique advantages that can complement the parameter space for high-temperature magnetic confinement plasma research. As a complement to existing RFP experimental devices, KTX aims to continuously increase its plasma current. By clarifying the self-organization process, KTX seeks to explore RFP’s feasibility as a fusion reactor.

2. UPGRADE OF POWER SUPPLY SYSTEMS

2.1. Ohmic field power supply

The Ohmic heating system serves as the main method for heating and driving the toroidal plasma current in the Keda Torus eXperiment (KTX) Reversed Field Pinch (RFP) device. The original Ohmic field power supply employed a two-stage capacitor design, consisting of a high-voltage capacitor bank for the plasma current ramp-up phase and a low-voltage bank for extending the current flat-top. While this design is feasible for conventional tokamak configurations, it proved to be a limiting factor for KTX's RFP operation. The high loop voltage required for Ohmic heating during the current start-up phase was incompatible with the low voltage provided by the second-stage capacitor bank, which prevented the bank from being engaged. To enable discharges with larger plasma currents and extended pulse durations, it was necessary to upgrade the system with a multi-stage capacitive inductive heating approach.

The upgraded Ohmic field power supply system was designed to address these limitations while meeting the specific operational requirements of the RFP configuration. The system's architecture is based on a modular, distributed topology, where the Ohmic field power supply is divided into three separate groups to reduce the voltage stress on the components and enhance insulation capabilities. These three power supply groups are connected in series with the three corresponding sections of the Ohmic field coils. Subsequent full system integration and optimization of discharge parameters, including the Ohmic field power supply, led to the successful achievement of a plasma current exceeding 500 kA in ultra-low q configuration. The waveforms from this successful discharge show the Ohmic coil current rising to over 4 kA and the loop voltage providing the necessary driving force for the plasma current to ramp up and then decay, confirming the overall success of the Ohmic power supply upgrade.

2.2. Feedback control system

The feedback control system on KTX is a multi-faceted system designed to address different types of plasma instabilities. It consists of two primary control loops: one for suppressing error fields at the vertical gaps and

another for mitigating magnetohydrodynamic (MHD) instabilities using an array of saddle coils. Both loops utilize an advanced electronics system based on Field-Programmable Gate Arrays (FPGAs) to achieve real-time control with high precision and low latency.

2.2.1. Real-Time Control Architecture

The core of the KTX feedback system is a flexible, distributed, real-time control system built around FPGAs. This architecture was chosen for its ability to perform parallel operations, offering performance that is at least an order of magnitude superior to traditional general-purpose processors (GPPs). The system is composed of several key elements: detectors, real-time electronics, and actuators.

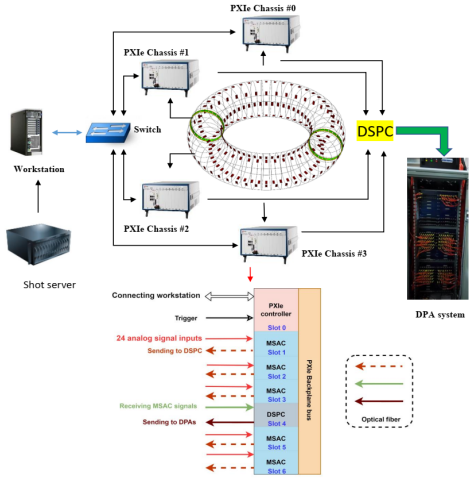

Fig.1 Overall logic block diagram of the active feedback control coils

The detection system uses a variety of sensors to acquire data from the plasma edge. These include saddle sensors, 2D electromagnetic probes (EMPs), and Rogowski probes. The saddle sensors, arranged in a 4×26 matrix, detect the average localized radial magnetic field, with a toroidal mode number resolution of 12 and a poloidal resolution of 2. The EMPs measure poloidal and toroidal magnetic fields on the inner and outer surfaces of the composite shell, enabling the measurement of magnetic field fluctuations with poloidal modes $|m| \leq 2$ and toroidal modes $|n| \leq 23$.

The data from the sensors are then fed into a distributed real-time electronics system housed in four PXI Express (PXIe) chassis. Each chassis contains multiple custom-developed multi-channel signal acquisition cards (MSACs) and data summary processing cards (DSPC). An FPGA acts as the central processor for each card, handling real-time data acquisition, calculation, and feedback generation. This FPGA-based design is the first of its kind used for real-time MHD control in KTX, fully meeting the experiment's real-time requirements with a total response time of less than 50 μs. The actuators consist of Digital Power Amplifiers (DPAs) and saddle coils. The real-time control system sends a reference signal to the DPAs, which then drive current through the saddle coils. These coils, firmly mounted on the outer surface of the KTX's passive shell, generate the feedback magnetic field to counteract instabilities in the plasma. The DPAs operate at a frequency of up to 25 kHz, and each one is independently controlled, allowing for the creation of disturbed magnetic field modes with poloidal numbers $|m| \leq 2$ and toroidal numbers $|n| \leq 12$.

2.2.2. Error Field and MHD Instability Control

The KTX feedback system is specifically designed to address two primary types of magnetic perturbations: static error fields and dynamic MHD instabilities. Imperfections in device construction, such as poloidal gaps in the stabilizing shell, can create an unwanted static or slowly varying magnetic field known as the error field. This field can severely degrade plasma confinement and lead to premature discharge termination. The KTX utilizes a compound control method that combines passive and active techniques to mitigate this issue. Active control is achieved through an array of 32 error field control coils located at the two poloidal gaps. These coils, driven by dedicated DPAs, generate a compensating magnetic field to reduce the local error field. Open-loop control experiments have demonstrated that this system can reduce the dominant m=1 error field component by over 90%.

This has resulted in a 50% increase in plasma current and a 30% increase in discharge duration during the later stages of the discharge. RFP devices, including KTX, are susceptible to various MHD instabilities like resistive wall modes (RWMs) and tearing modes (TMs). These instabilities can grow and lead to the premature termination of plasma discharges. The second part of the feedback system is dedicated to controlling these dynamic instabilities. It uses a 4×12 array of saddle coils, driven by 48 DPAs, to apply a real-time feedback magnetic field to the plasma boundary. Simulations and experiments have shown that this system can effectively stabilize RWMs by suppressing their growth and even driving them to rotate, which is a key strategy for improving plasma confinement.

The KTX control system has employed various control methodologies to optimize performance. A key approach has been the use of Proportional-Integral-Derivative (PID) control, a well-known and widely implemented control strategy. To enhance control performance, a cascade PID control scheme has been implemented. This dual-layered structure includes an inner loop for regulating the current in the saddle coils and an outer loop for controlling the magnetic field at the plasma boundary. The Inner Model Control (IMC) method was chosen to tune the PID parameters, as it simplifies the tuning process by reducing the number of free parameters. Simulations confirmed that the IMC-tuned cascade PID controller provides a faster response and better control over overshoot and damping compared to other methods like the Ziegler-Nichols (Z-N) method.

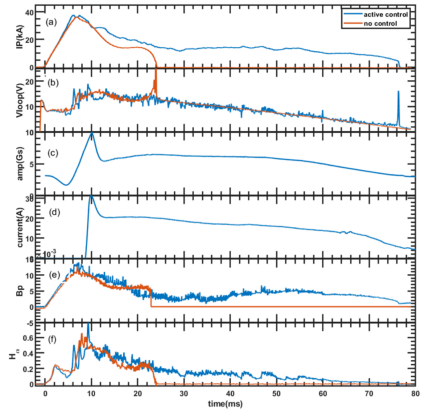

Fig.2 Comparison of long-pulse discharges with and without active control: (a) Plasma current waveform; (b) Loop voltage; (c) (1,0) magnetic field amplitude; (d) Active feedback (1,0) current amplitude waveform; (e) Poloidal magnetic field waveform; (f) Hα waveform.

The successful application of the feedback control system in KTX has yielded promising experimental results. Experiments have shown that active feedback control can extend the plasma discharge duration from 24 ms to an impressive 76 ms. In a particularly successful experiment, a plasma discharge time of 104 ms was achieved. This was accomplished by suppressing the dominant (1,0) mode instability with PID closed-loop feedback control. The system has proven effective not only in mitigating instabilities but also in improving overall plasma parameters like plasma current and loop voltage.

3. AUXILIARY CONTROL SYSTEMS

A range of auxiliary control systems have been developed and applied to control plasma parameters, including an electron cyclotron wave heating system for non-inductive pre-ionization, biased electrodes for controlling the boundary electric field, and a compact torus for localized fueling.

3.1. Electron cyclotron wave

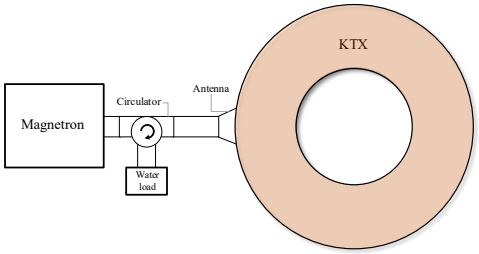

Fig.3 The main components of the microwave transmission path

The entire pre-ionization system consists of three key components: the magnetron, the transmission waveguide and antenna, and the supporting power supply and water-cooling system. The core magnetron for the KTX microwave system produces 2450 MHz electromagnetic waves. This frequency is based on Electron Cyclotron Resonance (ECR) calculations, corresponding to an 875 Gs longitudinal magnetic field, compatible with the ~0.1 T KTX discharge field. Operating at 12.6 kV and 1.8 A, the magnetron delivers 3–15 kW power at 2450±30 MHz, with ±3% stability at full power. The microwave is typically activated before discharge. Figure 4 shows a typical comparison of discharges with and without pre-ionization. The use of ECW for pre-ionization significantly improves the breakdown phase. Compared to discharges without ECW assistance, both the breakdown voltage and time are substantially reduced—from 72 V to 52 V and from 0.652 ms to 0.060 ms, respectively. This reduction effectively decreases the volt-second consumption of the ohmic field.

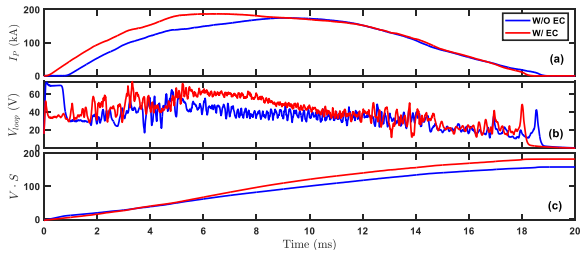

Fig.4 The comparison of (a) plasma current, (b) loop voltage, and (c) volt-second consumption under conditions with and without microwave injection.

3.2. Biased electrodes.

Suppressing turbulence is critical for improving plasma confinement and necessitates control over the electric field or current profile. A key tool for this purpose is the use of biased electrodes. To this end, two independent biased electrode systems were designed and installed on KTX to manipulate the edge electric field and the edge parallel current profile. The graphite electrodes (35 mm diameter) are radially movable. Current profile modification requires a total driven current up to 10 kA. Two high-power pulse supplies (±300 V/3000 A and ±1000 V/3000 A), controlled by IGBT H-bridges, power the electrodes.

In edge radial electric field control experiments conducted in a tokamak configuration, the biased electrode was successful in altering the edge radial electric field. Under bias, there was an accompanying increase in electron density and plasma duration. However, both electrostatic and magnetic fluctuations were enhanced. A significant peak in the magnetic signal was observed at 23.4 kHz (suspected to be an m/n=2/1 tearing mode), and another peak was detected in both potential and magnetic signals at 7.8 kHz (possibly an m/n=4/1 tearing mode). The mechanism behind this enhancement is currently unclear and requires further investigation. In edge parallel current profile control experiments performed in an RFP configuration, the two biased electrodes enabled local plasma to reach a deeper reversed field state and achieve higher densities by modifying the edge parallel current profile. A reduction in the amplitude of magnetic fluctuations was observed within the reversed field enhanced region, suggesting that the biased electrodes have a suppressive effect on magnetic perturbations. While the electrostatic fluctuations did not show a significant reduction, this may be due to the probe's position being outside the region most influenced by the electrode. These findings underscore the effectiveness of biased electrodes in controlling both the edge radial electric field and the edge parallel current profile, which is vital for enhancing plasma confinement in RFPs.

3.3. Compact torus injection

Research on the Keda Torus eXperiment (KTX) device is actively exploring the use of Compact Torus Injection (CTI) as a promising method to address critical issues in Reversed Field Pinch (RFP) plasmas, such as fueling and current sustainment. The KTX-CTI system aims to provide an efficient deep fueling mechanism and to investigate the impact of compact torus (CT) injection on plasma performance.

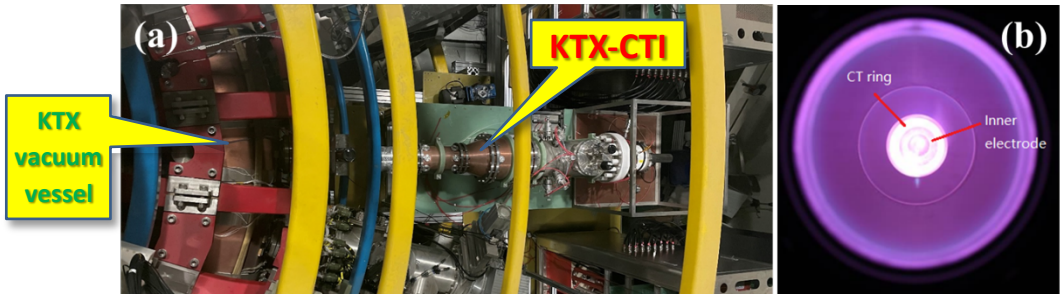

Fig.5 (a) KTX-CTI installed on KTX and (b) CT discharge ring photoed by visible light camera

The system's design is specifically tailored to generate CTs with high density and velocity, enabling them to overcome the pressure in plasma and achieve deep fueling. To precisely measure the key parameters of the CT plasma, a multi-channel Optical Fiber Interferometer (OFI) was used to measure the line-integrated electron densities of the CT. The peak electron density of CT is approaching $10^{22}m^{-3}$. The axial exit velocity of the CT can be inferred to be about 300 km/s, based on the time difference of their peaks.

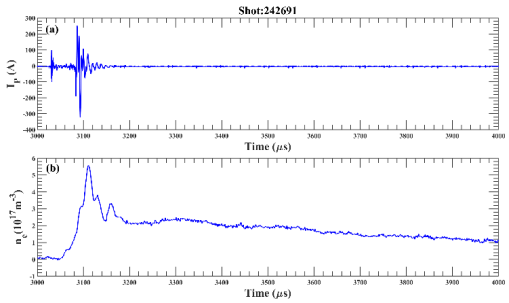

Fig.6 Induced current correlated with helicity injected, and electron density peak by CT injected into KTX vacuum vessel with toroidal magnetic field

Initial experiments using the KTX-CTI system on the KTX device have yielded significant results, highlighting the potential of CT injection for fusion applications. It is demonstrated that the CT successfully penetrated the toroidal magnetic field and reached the inner wall of the KTX vacuum vessel. Density measurements showed a rapid increase in plasma density across all five radial channels, with the highest peak near the inner wall, confirming successful deep fueling. The intrinsic helicity of the CT was shown to induce a modest KTX plasma current of 200 A, consistent with predictions based on helicity conservation. This capability was further demonstrated as a viable pre-ionization and current start-up technique, with CT injection successfully initiating a normal plasma discharge at a low loop voltage of approximately 20 V without the use of gas puffing. Injection of a CT into an RFP discharge resulted in a rapid increase in central density, with the peak density reaching $2.43\times10^{19}m^{-3}$, a value 1.3 times the Greenwald density limit. The density profile became more peaked after injection, suggesting that the majority of the injected particles were predominantly confined within the core of the KTX plasma. The central density then decayed with a time constant consistent with the particle confinement time of the RFP plasma, demonstrating the effectiveness of CT injection for density modulation and for exploring density limits in fusion devices.

4. EXPERIMENTAL OPERATION

With upgraded OH power supply and modified connection of the toroidal field coil to reduce its self-inductance, aided reversal mode discharge is realized on KTX.

4.1. RFP discharge in MH state

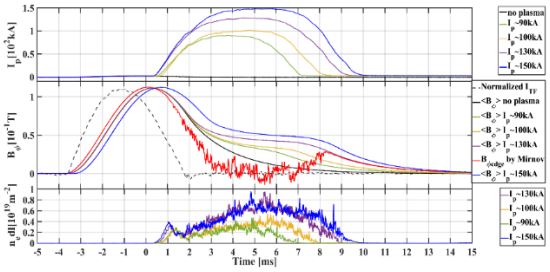

Fig.7 Aided reversal mode discharge waveforms of plasma currents, toroidal magnetic field and central chord-integrated density

The theoretical requirement for a rapid current ramp in the aided-reversal mode stems from the magnetic configuration during this initial phase. Since the externally applied toroidal magnetic field is substantially larger than the eventual field in the formed RFP state, the safety factor profile (q-profile) resides between that of a tokamak and a final RFP. This intermediate configuration is often ideal MHD unstable. Therefore, a high loop voltage is required to drive a fast current increase, thereby minimizing the duration of this unstable phase and preventing both magnetic flux and power consumption losses.

As shown in the figure 7, the externally applied toroidal field was optimized by adjusting the toroidal field coil connections to achieve a falling edge time of 3 ms. Due to the vacuum vessel's magnetic field penetration time (2 ms), the actual internal field (solid line, measured by internal probes) exhibits a slight delay. The boundary measurement shows a fluctuating edge toroidal field, while the single-turn toroidal flux loop measures a smoother averaged field. Significantly, increasing the loop voltage successfully elevates the plasma current, and the corresponding averaged toroidal field remains at a higher level, even after the externally applied field has dropped to zero. This sustained internal toroidal field is a classic manifestation of RFP plasma self-organization, where a poloidal current is intrinsically generated to maintain the internal magnetic flux. From the reconstructed equilibrium profile during the discharge, it is more obvious that the magnetic field and current density distribution exhibit typical RFP characteristics.

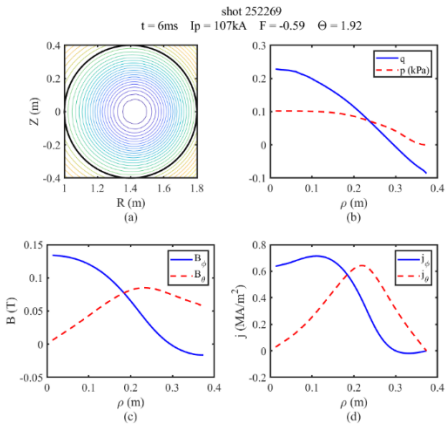

Fig.8 (a) Poloidal flux surfaces, (b) profiles of safety factor and pressure, (c) profiles of poloidal magnetic field and toroidal magnetic field, (d) profiles of toroidal current density and poloidal current density from equilibrium reconstruction in RFP discharge

4.2. Equilibrium improvement

The plasma equilibrium in KTX is controlled by equilibrium field (EF) coils. In the original design, six sets of EF coils shared the same power supply with the Ohmic field (OH) coils. However, experiments revealed that this configuration generated an excessively strong vertical field, causing the plasma to strike the inner wall. After experimental tests, we eventually adopted a configuration in which only two sets of EF coils were used. These coils were not directly powered; instead, their currents were induced by the OH coils. In this case, the currents in the OH coils, EF coils, and plasma can be approximately regarded as linearly related, ensuring that an appropriate vertical field can be provided for discharges under various operational conditions.

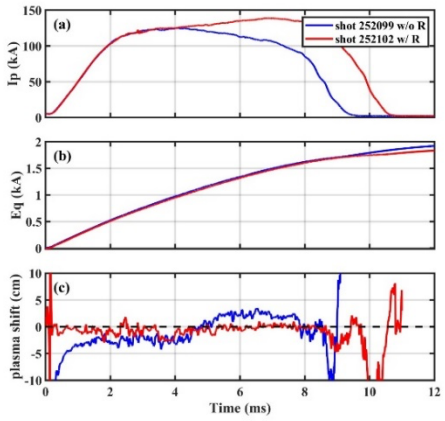

Fig. 9 Waveforms of (a) plasma current, (b) equilibrium field coil current, and (c) plasma centroid displacement during discharges with (red) and without (blue) resistors connected to the equilibrium field coils.

On this basis, adjustable resistors were connected in series with the EF coils, allowing the vertical field strength to be tuned according to specific discharge conditions. The results are shown in Figure 9, which demonstrates that with resistors, the plasma centroid remains stable during the discharge phase, indicating better plasma equilibrium, whereas without resistors, the plasma centroid exhibits significant displacement. In future work, we plan to connect the EF coils to active power supplies in order to realize real-time vertical field feedback, thereby achieving improved plasma equilibrium control.

5. UPGRATED DIAGNOSTIC SYSTEMS

5.1. Multi-channel polarization interferometer

The development of the terahertz-based solid-state source diagnostic system on the KTX device progressed from an initial compact interferometer to advanced polarimeter-interferometer systems, used for plasma equilibrium reconstruction and fluctuation studies.

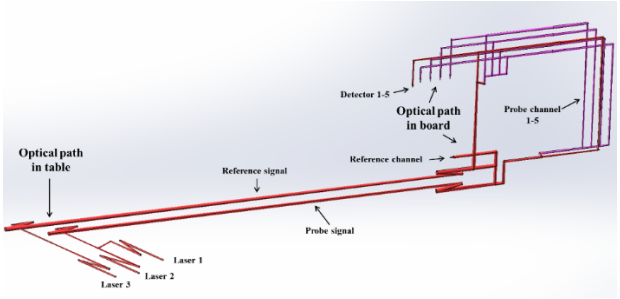

Fig.10 Schematic diagram of the optical path for upgraded multi-channel polarimeter-interferometer from the original interferometer system

To address strong stray magnetic and electric fields from the air core coils, which induce vibrations in metal components, a lightweight and stable support platform was crucial. The platform was constructed from non-

metallic epoxy resin and mounted on sand-filled stainless-steel pillars to eliminate electromagnetically-induced vibrations. Replacing commercial metal optical mounts with non-metallic ones and adding mechanical reinforcements successfully reduced vibration-induced phase shift to background noise levels. A subsequent multi-channel terahertz solid-state interferometer was installed on KTX, utilizing two solid-state sources at ~650 GHz with ~2 mW output power each. The optical design ensured uniform power distribution and a reduced beam width (~20 mm across the plasma) to minimize crosstalk and energy loss. This system, with a phase noise of ~0.0047, successfully measured electron density profiles and fluctuations. The interferometer was also used for collective forward scattering measurements to study electron density fluctuations, a technique that allows simultaneous measurement of chord-averaged density and fluctuations. Its sensitive Schottky planar diode mixer detected forward scattering signals even with low source power, revealing high-frequency modes (up to 50 kHz) relevant for turbulence analysis.

Building on this, a polarimeter-interferometer system was developed for the simultaneous measurement of both electron density and the Faraday rotation angle (which provides internal magnetic field information). This system uses a "three-wave" technique with a third terahertz source, offering compactness. The system, designed with three vertical channels, demonstrated low phase noise for both Faraday effect (<0.8◦) and density (<0.9◦), proving the capability of the solid-state sources for these fusion diagnostics.

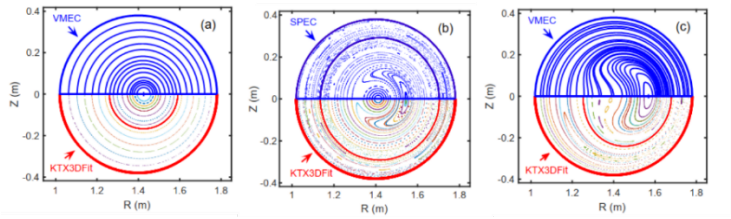

Fig.11 Equilibrium reconstruction results constrained by simulated diagnostic data from a polarimeter-interferometer under (a) toroidal symmetric equilibrium, (b) a bi-axial helical state calculated by the SPEC code, and (c) a quasi-single helical state calculated by the VMEC code

The polarimeter-interferometer data is a key input for the new 3D equilibrium reconstruction code, KTX3DFit. This code, based on the multi-region relaxed magnetohydrodynamic (MRxMHD) model and the stepped-pressure equilibrium code (SPEC), is designed to reconstruct complex 3D plasma states, including those with magnetic islands. Simulations using KTX3DFit confirmed the diagnostic's ability to distinguish between axisymmetric, double-axis helical (DAx), and single-helical-axis (SHAx) states, showing high consistency with other numerical codes. This integration marks the first use of internal magnetic field data with the SPEC code for equilibrium reconstruction.

Future work involves upgrading the system to more channels for higher spatial resolution to better capture smaller-scale magnetic island structures. The upgraded system will be used to investigate the relationship between density/magnetic field fluctuations and MHD instabilities and to reconstruct the evolution of 3D plasma equilibrium during state transitions (MH to QSH) using real experimental data.

5.2. Double-foil soft x ray detection arrays

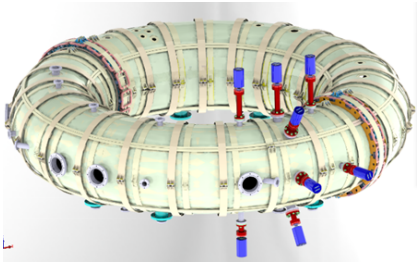

Fig.12 Schematic diagram of the layout of the 8 soft X-ray probe diagnostic systems on KTX

The Double-foil Soft X-ray (SXR) Array Imaging diagnostic (DSXAI) on KTX is designed for core plasma physics studies, especially in the quasi-single-helicity (QSH) state characteristic of Reversed Field Pinches (RFP).

This advanced system integrates tomographic reconstruction with a double-foil technique to provide comprehensive, two-dimensional profiles of both bremsstrahlung emissivity and electron temperature (Te). The DSXAI system comprises eight subsystems with a total of 320 channels, enabling high-resolution plasma imaging. Each subsystem includes two different metal foils (aluminum, 0.8–7.2 μm thick), an aperture slit, an photodiode array, and high-speed amplifiers.

The system's design was rigorously optimized using the Bayesian Experimental Design (BED) approach to maximize information gain about key plasma parameters, such as the emissivity axis shift. The final configuration of eight subsystems across three toroidal locations, with camera pairs separated by 90° toroidally, was chosen for stable reconstructions. The optimal camera opening angle is 96° with 17 sightlines per camera. The hardware ensures both sensitivity and speed: the AXUV photodiodes have a fast response time of 200 ns, and the high-transimpedance amplifiers (1×10^7 V/A) provide a system bandwidth of 50 kHz. Initial experiments confirmed all 320 channels are operational with good signal-to-noise ratio. The diagnostic has an estimated spatial resolution of 4–5 cm and a time resolution of ~20 μs. While the initial low Te in KTX made the double-foil Te measurement challenging, the system is ready for reconfiguration as KTX's operational parameters advance.

DSXAI will be instrumental in studying QSH dynamics, imaging helical structures, and investigating the relationship between magnetic topology and plasma confinement as KTX moves toward higher currents and temperatures.

6. STUDY OF HELICITY

Magnetic helicity, a fundamental physical quantity describing the topological properties of magnetic field lines, such as their linking and twisting, plays a crucial role in the self-organization of plasmas in Reversed Field Pinches (RFPs). Both experimental and numerical studies on the role of helicity in plasma equilibrium and stability have been carried out on KTX. Numerical simulations of self-organized states and the development of active control techniques for helicity injection would help providing comprehensive insights into helicity-related phenomena and operation improvement of RFP.

6.1. Simulation of helicity on RFP equilibrium

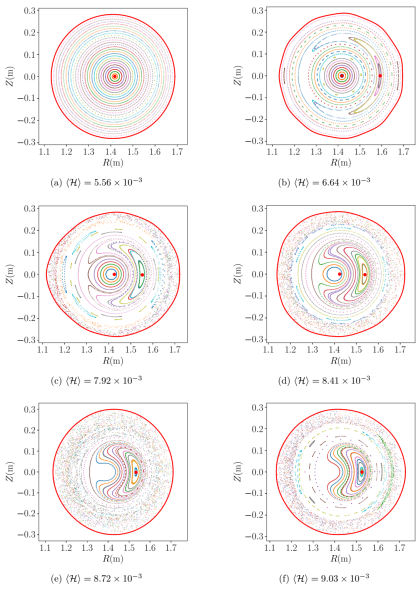

Fig.13 Poincaré cross section at $\zeta = 0$ of the magnetic field with different $\langle\mathcal{H}\rangle$.

Stepped-pressure equilibrium code (SPEC) is applied for numerically modeling the different self-organized states in KTX, which is based on the multi-region relaxed magnetohydrodynamic (MRxMHD) model. This model partitions the plasma volume into subvolumes with conserved magnetic helicity, allowing for the simulation of complex three-dimensional (3D) equilibria without the assumption of nested magnetic surfaces. The simulations identified a strong relationship between the plasma's core magnetic helicity density and the resulting self-

organized state. At low helicity densities, the plasma exhibits an axisymmetric state. As the core helicity increases, the plasma undergoes a spontaneous transition to more complex 3D helical states. The study demonstrates a bifurcation from the axisymmetric state to a double-axis (DAx) state, characterized by two twisted magnetic axes, when the helicity exceeds a threshold of $5.84\times10^{-3}\mathrm{T}^{-2}\mathrm{m}$. A further increase in helicity leads to a transition to a single-helical-axis (SHAx) state, a phenomenon observed in other RFP devices and a state associated with improved confinement. The numerical results predict that KTX can achieve a DAx state with a plasma current above 0.6 MA and a SHAx state at approximately 0.72 MA, consistent with a linear relationship found between plasma current and core helicity.

Further analysis of the helical states revealed a dominant m=1, n=6 Fourier component of the magnetic field at the plasma edge, which becomes more pronounced with increasing helicity. The simulations also showed that the magnetic shear in the core vanishes in the DAx and SHAx states, indicating the formation of large magnetic islands or helical flux tubes. Helicity decomposition analysis highlighted that the total helicity is primarily composed of the self-helicity of these flux tubes, with twisting helicity being the dominant component in the old flux tube and writhing helicity contributing significantly to the new, 3D helical flux tube.

6.2. Measurement of helicity flow on KTX

The measurement of magnetic helicity in KTX is grounded in the helicity evolution equation, which links changes in the total plasma helicity to dissipation and transport across the plasma boundary. For a gauge-invariant description, the relative helicity within a plasma volume is the key quantity of interest. Its time evolution is governed by $dH_R/dt = -2\int_{V_p}\eta J\cdot BdV - \oint_{S_p}[(A_{pc}\times E)\cdot dS + \mu_0(\psi_{pc}A_{pc})\cdot dS]$,The first term on the right-hand side represents helicity dissipation due to plasma resistivity η. The second term describes the helicity flux across the plasma boundary S_p. In this formulation, E is the electric field and B is the magnetic field, while A_{pc} is the vector potential of a reference field and ψ_{pc} is its magnetic scalar potential. The key to experimental measurement lies in quantifying the helicity flux term, which is the net helicity entering or leaving the plasma from the boundary. This approach is powerful because it allows for helicity measurement without needing to solve the complex volume integral of the helicity density throughout the plasma, instead focusing on the more experimentally accessible boundary parameters.

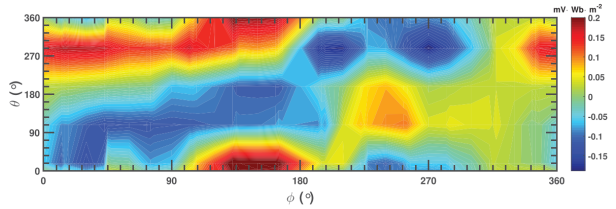

Fig.14 The high-frequency fluctuating magnetic helicity flux density (MHFD) is shown in a $\theta-\phi$ plane

The experimental validation of this theory hinges on a suite of high-performance diagnostics on KTX that measure the necessary electric and magnetic field components at the plasma boundary. These diagnostics are designed with the high spatial and temporal resolution required to capture the dynamics of MHD instabilities and the subtle effects of helicity injection. The cornerstone of helicity flux measurement on KTX is the eddy-current diagnostic system. This innovative system leverages the device's conductive copper shell to act as a natural sensor for boundary electric fields. When the plasma's magnetic field changes, it induces eddy currents in the nearby shell, which are directly proportional to the tangential electric field at the boundary. The system comprises a dense array of magnetic probes and saddle loops placed both on the inner and outer surfaces of the copper shell. These probes measure the differential magnetic fields across the shell, allowing for the calculation of the eddy currents. According to Ampère's circuital law, the magnetic field jump across the thin copper shell is related to the current flowing within it. By measuring the magnetic field components with the probe arrays, the system can determine the magnitude and distribution of eddy currents on the shell surface. The eddy current density j on the shell is directly related to the tangential electric field E_t by the shell's conductivity σ_{shell} via Ohm's law: $j=\sigma_{shell}E_t$. Thus, by measuring the eddy currents, the system effectively quantifies the boundary electric field, a key parameter for the helicity flux calculation. The high sensitivity of this system is particularly important for KTX, as small electric field perturbations can drive significant eddy currents on the low-resistivity copper shell. The

system is capable of measuring both the poloidal and toroidal components of the eddy currents, providing a complete picture of the boundary helicity flux vector.

KTX employs a vast array of EMPs (up to 320 two-dimensional probes) installed inside the vacuum vessel and on the outer surface of the copper shell. These probes provide high-resolution measurements of the magnetic field's poloidal and toroidal components. The data from these probes are crucial for mode decomposition. An array of 104 single-turn saddle sensors is mounted on the outer surface of the vacuum vessel to specifically measure the radial magnetic field. These sensors are a critical part of the feedback control system, as they provide a direct, real-time input signal for the controller to act upon. The radial field is often the most important component of an instability, so its accurate measurement is crucial for effective suppression.

With the eddy-current diagnostic system, the helicity flux entering the plasma from the boundary has been quantified. For a typical discharge with a plasma current of around 200 kA, the measured helicity flux density was found to be on the order of $10^{-3}Wb^2/s$. This value was consistent with the helicity needed to sustain the plasma current against resistive dissipation, as predicted by the Taylor relaxation model. On the other hand, the experimental data showed a clear correlation between the injected helicity flux and the plasma's response. The measurement of the helicity flow was used to calculate the helicity injection rate, which was then compared to the change in plasma current. It was found that in discharges where a net helicity flux was measured, the plasma current was either sustained or increased, while in discharges with low or zero net flux, the current decayed. This direct correlation provided strong experimental evidence that helicity injection is an effective mechanism for sustaining the plasma current.

7. SUMMARY

KTX has undergone significant upgrades to enhance its operational capabilities, supporting in-depth research on RFP physics. The major enhancements include an upgraded Ohmic field power supply which has achieved high-current discharges over 500 kA and the implementation of a boundary magnetic field feedback control system. Auxiliary control systems further aid operation capabilities for KTX, including: an ECW system, two sets of biased electrodes a CTI system. The Aided-Reversal mode is achieved by a high loop voltage drive to quickly pass through the ideal MHD unstable intermediate configuration. New diagnostics, including the terahertz polarimeter-interferometer and the DSXAI system, provide key data for studying plasma instabilities and for the 3D equilibrium reconstruction code KTX3DFit. Numerical simulations support these efforts by exploring the maintenance mechanisms of the QSH state, highlighting the role of helicity in magnetic topology and self-organization.

ACKNOWLEDGEMENTS

This work was supported by National Natural Science Foundation of China (Nos. 12175227, 12375226, and 12405268), the National Magnetic Confinement Fusion Program of China (No.2024YFE03130003 and 2022YFE03100004), and the Strategic Priority Research Program of the Chinese Academy of Sciences under Grant No. XDB-0790300.

REFERENCES

[1] LIU, Wandong, et al., Nuclear Fusion 57 (2017): 116038.
[2] TAO, Zhen, et al., Fusion engineering and design 195 (2023): 113968.
[3] CHEN, Zheng, et al., Plasma Physics and Controlled Fusion 65.12 (2023): 125008.
[4] TAO, Zhen, et al., Fusion Engineering and Design 206 (2024): 114592.
[5] Jiaren, W. U., et al., Plasma Science and Technology 27.4 (2025): 044005.
[6] LAN, Tao, et al., Plasma Science and Technology 26.10 (2024): 105102.
[7] WANG, Xingkang, et al., Plasma Science and Technology 26.3 (2024): 034009.
[8] LIU, Ke, et al., Nuclear Fusion 64.5 (2024): 056037.
[9] ZU, Yiming, et al., Plasma Physics and Controlled Fusion 64.6 (2022): 065002.
[10] HUANG, Yuhua, et al. , Plasma Science and Technology 26.12 (2024): 125104.